Title

Cleft palate defect of Dlx1/2−/− mutant mice is caused by lack of vertical outgrowth in the posterior palate

Journal

Developmental Dynamics, 241(11)

ISSN

1058-8388

Authors

Jeong, Juhee
Cesario, Jeffry
Zhao, Yangu
et al.

Publication Date

2012-11-01

DOI

10.1002/dvdy.23867

Peer reviewed

Published in final edited form as:
Dev Dyn. 2012 November ; 241(11): 1757–1769. doi:10.1002/dvdy.23867.

Cleft Palate Defect of *Dlx1/2*$^{-/-}$ Mutant Mice is Caused by Lack of Vertical Outgrowth in the Posterior Palate

Juhee Jeong[1,*], **Jeffry Cesario**[1], **Yangu Zhao**[2], **Lorel Burns**[1], **Heiner Westphal**[2], and **John L. R. Rubenstein**[3,*]

[1]Department of Basic Science and Craniofacial Biology, New York University College of Dentistry, New York, NY

[2]Laboratory of Mammalian Genes and Development, Program on Genomics of Differentiation, Eunice Kennedy Shriver National Institute of Child Health and Human Development, Bethesda, MD

[3]Department of Psychiatry, Nina Ireland Laboratory of Developmental Neurobiology, University of California, San Francisco, CA

Abstract

Background—Mice lacking the activities of *Dlx1* and *Dlx2* (*Dlx1/2*$^{-/-}$) exhibit cleft palate, one of the most common human congenital defects, but the etiology behind this phenotype has been unknown. Therefore, we analyzed the morphological, cellular, and molecular changes caused by inactivation of *Dlx1* and *Dlx2* as related to palate development.

Results—*Dlx1/2*$^{-/-}$ mutants exhibited lack of vertical growth in the posterior palate during the earliest stage of palatogenesis. We attributed this growth deficiency to reduced cell proliferation. Expression of a cell cycle regulator *Ccnd1* was specifically down-regulated in the same region. Previous studies established that the epithelial-mesenchymal signaling loop involving Shh, Bmp4 and Fgf10 is important for cell proliferation and tissue growth during palate development. This signaling loop was disrupted in *Dlx1/2*$^{-/-}$ palate. Interestingly, however, the decreases in *Ccnd1* expression and mitosis in *Dlx1/2*$^{-/-}$ mutants were independent of this signaling loop. Finally, *Dlx1/2* activity was required for normal expression of several transcription factor genes whose mutation results in palate defects.

Conclusions—The functions of *Dlx1* and *Dlx2* are crucial for the initial formation of the posterior palatal shelves, and that the *Dlx* genes lie upstream of multiple signaling molecules and transcription factors important for later stages of palatogenesis.

Keywords

Dlx; cleft palate; palatogenesis; craniofacial development; mice

[*]Authors for correspondence. Juhee Jeong, 345 E. 24th street, Room 902D, New York University College of Dentistry, New York, NY 10010, USA, Tel) 212-992-7146, Fax) 212-995-4204, jj78@nyu.edu, John L. R. Rubenstein, 1550 4th street, Room 284C, University of California, San Francisco, CA 94158, USA, Tel) 415-476-7862, Fax) 415-476-7884, john.rubenstein@ucsf.edu.

Introduction

Dlx family genes encode homeodomain transcription factors with homology to the *Drosophila Distal-less* gene (Panganiban and Rubenstein, 2002). There are six *Dlx* genes in mammalian genome, *Dlx1* through *Dlx6*, arranged as three tightly linked pairs (*Dlx1/2, Dlx3/4* and *Dlx5/6*) (Porteus et al., 1991; Price et al., 1991; Robinson and Mahon, 1994; Simeone et al., 1994). Analyses of mice with targeted mutations have revealed that *Dlx* genes play crucial roles in development of multiple body parts including the forebrain, limb and jaw (Qiu et al., 1995, 1997; Anderson et al., 1997; Acampora et al., 1999; Depew et al., 1999, 2002; Beverdam et al., 2002; Merlo et al., 2002; Panganiban and Rubenstein, 2002; Robledo et al., 2002; Robledo and Lufkin, 2006; Jeong et al., 2008). All six of the mammalian *Dlx* genes are expressed in the embryonic primordium of the jaw, called the first pharyngeal arch (PA1), primarily in the neural crest-derived mesenchyme but also in specific areas of the ectoderm (Dollé et al., 1992; Bulfone et al., 1993; Robinson and Mahon, 1994; Simeone et al., 1994; Qiu et al., 1997). PA1 comprises two domains; the maxillary arch (mxPA1), which is the prospective upper jaw, and the mandibular arch (mdPA1), the prospective lower jaw. *Dlx1* and *Dlx2* are expressed broadly in both mxPA1 and mdPA1, while the expression of *Dlx3, Dlx4, Dlx5* and *Dlx6* is confined to mdPA1. This nested pattern of *Dlx* expression is thought to be crucial in differentiating the lower jaw versus upper jaw fate within PA1 (Beverdam et al., 2002; Depew et al., 2002).

Targeted mutations in mice of *Dlx1* and/or *Dlx2*, the focus of this paper, resulted in an abnormal upper jaw (Qiu et al., 1995, 1997); the lower jaw appeared unaffected, likely due to functional compensation by other *Dlx* genes. In $Dlx1^{-/-}$ mutants, the ala temporalis (connection of the skull base to the temporal wall) was hypoplastic (Qiu et al., 1997). $Dlx2^{-/-}$ mutants had more extensive defects including severe reduction of the ala temporalis, fragmentation and hypoplasia of the squamosal bone and zygomatic arch on the temporal wall, dysmorphic incus, appearance of ectopic cartilage, and hypoplasia and partially penetrant clefting of the secondary palate (Qiu et al., 1995). Mice with deletions in both *Dlx1* and *Dlx2* ($Dlx1/2^{-/-}$) showed exacerbation of the $Dlx2^{-/-}$ phenotype indicative of functional overlap between *Dlx1* and *Dlx2*. Defects in $Dlx1/2^{-/-}$ mutants included fully penetrant cleft secondary palate and loss of upper molars (Qiu et al., 1997; Thomas et al., 1997).

Cleft palate is a relatively common congenital defect in humans, affecting approximately 1 out of 700 births (Tolarova et al., 1998; Dixon et al., 2011). Normal development of the palate (palatogenesis) involves precise coordination of growth and morphogenesis of orofacial tissue, which appears to be easily perturbed by genetic and environmental factors (Ferguson, 1988; Gritli-Linde, 2007, 2008; Dixon et al., 2011; Bush and Jiang, 2012). In mice, the secondary palate begins to develop around embryonic day (E) 11.5, when the palatal shelves emerge from the internal side of mxPA1. The palatal shelves grow vertically along the sides of the tongue (E11.5 – E13.5), elevate above the tongue into a horizontal position (E14.0), grow towards the midline, where they meet and adhere to each other (E14.5). Finally, the epithelial seam between the shelves disintegrates to complete their fusion (E16.5). Over 200 mouse lines with mutation(s) in one or more genes exhibit cleft palate phenotype (Iwata et al., 2012), and detailed analyses of cellular and gene expression

changes in some of these mutants have been instrumental in elucidating signaling and genetic pathways regulating palatogenesis (Gritli-Linde, 2007, 2008; Bush and Jiang, 2012). However, in most of these mutants, palate development was affected only after it had progressed substantially (E13 or later), and thus the analyses focused on mid to late stages (E12.5 – E14.5). Therefore, molecular regulation of the initial steps of palatogenesis (around E11.5) remains poorly understood.

Although it was reported almost fifteen years ago that mouse *Dlx1/2*$^{-/-}$ mutants had cleft secondary palate (Qiu et al., 1997), nothing was known about the molecular and cellular etiology behind this phenotype. In fact, given that these mutants suffer from structural defects in a broad region of the face (Qiu et al., 1997), it was not even known whether the cleft palate was due to problems intrinsic to the palatal shelves, or was indirectly caused by a mechanical hindrance due to dysmorphology of surrounding structures. To answer this question, we analyzed the morphological, cellular and gene expression changes in the developing palate caused by inactivation of *Dlx1* and *Dlx2*. Our data show that the activities of *Dlx1* and *Dlx2* are important for the initial outgrowth of the palatal shelves in a region-specific manner, and are essential for the normal expression of other important regulators of palatogenesis.

Results

Dlx1 and *Dlx2* are expressed prior to and during early stages of palatogenesis but are down-regulated afterward

To identify the time window when *Dlx1* and *Dlx2* can potentially influence palatogenesis, we examined their expression from E8.5 to E13.5 at a high spatio-temporal resolution (Fig. 1). Expression of *Dlx2*, but not *Dlx1*, was detected at E8.5, in the nascent PA1 and in the area between the cranial neural crest (CNC) and PA1, presumably migrating CNC cells (Fig. 1A–D). *Dlx1* expression was first detected in PA1 at E9.0, and by E9.5, both genes were expressed in most of PA1 (Fig. 1E–H). From E10.5, we used a series of coronal sections of the head to examine *Dlx* expression along the A-P axis of the developing palate. At E10.5, shortly before the formation of the palatal shelves, *Dlx1* and *Dlx2* were expressed broadly in the mesenchyme of PA1 at the middle and posterior level (Fig 1K–N), including the prospective palate area (ventro-medial domain of mxPA1, Fig. 1I–N). However, at the anterior level, *Dlx* expression was confined to the lateral domain away from the prospective palate, mainly in the epithelium (Fig. 1I–J). A similar pattern continued at E11.5 in the nascent palatal shelves, although the expression levels were reduced in the nasal half (Fig. 1O–T). The palatal expression of the *Dlx* genes continued to diminish through E13.0 (Fig 1U–Z) and became almost undetectable by E13.5 (data not shown) except in the dental mesenchyme of the developing molars (Fig. 1W,X). These results were consistent with earlier reports on the expression of *Dlx1* and *Dlx2* (Dollé et al., 1992; Bulfone et al., 1993; Robinson and Mahon, 1994; Qiu et al., 1997). Based on these data, we inferred that *Dlx1* and *Dlx2* might be involved in the beginning of palate development, but unlikely to play any direct roles at later steps of palatogenesis.

Posterior palatal shelves fail to grow in *Dlx1/2*$^{-/-}$ mutants

To determine when the defects in palatogenesis first arise in *Dlx1/2*$^{-/-}$ mutants and how it progresses, we examined tissue morphology of the palate region in sections from E10.5 to E14.5 (Fig. 2). At E10.5, *Dlx1/2*$^{-/-}$ mutants exhibited hypoplasia of mxPA1; the tissue mass lateral to the eyes was grossly reduced (Fig. 2C,D). While striking, this phenotype most likely correlates with the defects in lateral facial structures, such as loss of zygomatic arch and hypoplasia of squamosal bone, rather than the cleft palate. Therefore, herein we did not investigate this phenotype, but rather focused on the palate, which arises from the ventro-medial domain of mxPA1.

At all stages examined, anterior palate was relatively normal in the mutants (Fig. 2). Although delay in anterior palatal shelf elevation was observed in some cases (Fig. 2S,T), it was likely to be an indirect consequence of more severe defects in the middle and posterior palate. At the middle level, the shape and cell density of the prospective palate region of mxPA1 appeared similar between the controls and mutants at E10.5 (Fig. 2C,D). When the palatal shelves formed at E11.5, the size (area measured in sections) of the mutant palatal shelves was 79% of the controls (Fig. 2I,J,Y; control: 0.064±0.003 mm^2, mutant: 0.050±0.004 mm^2). The size difference increased as development progressed, and at E14.5, the mutant palatal shelves failed to elevate above the tongue (Fig. 2O,P,U,V,Y).

The posterior palate was affected the most profoundly. At E10.5, the size of the mutant's prospective palate appeared normal (Fig. 2E,F) although in some mutants mesenchymal cell density appeared slightly lower. However, cell counting did not reveal a statistically significant difference in the posterior palate (control: 8588±915 cells/mm^2, mutant: 8348±753 cells/mm^2, p=0.744). On the other hand, by E11.5, the mutant palatal shelves were less than half (47.5%) the size of the controls (Fig. 2K,L,Y; control: 0.040±0.006 mm^2, mutant: 0.019±0.005 mm^2). Furthermore, while the control palatal shelves underwent rapid vertical growth between E11.5 and E13.5 (Fig. 2K,Q,Y), the mutant palatal shelves grew little (Fig. 2L,R,Y). By E14.5, the palatal shelves were essentially non-existent in the mutants at the posterior level (Fig. 2W,X).

In summary, the posterior palate suffered severe growth deficiency from the onset of the palatogenesis in *Dlx1/2*$^{-/-}$ mutants, while the anterior palate was largely spared. This difference in phenotype along the A-P axis is consistent with the lack of *Dlx1* and *Dlx2* expression in the anterior palate region (Fig. 1).

Cell proliferation and *Cyclin D1* expression are reduced in the posterior palate of *Dlx1/2*$^{-/-}$ mutants

To explain the growth deficiency of the palatal shelves of *Dlx1/2*$^{-/-}$ mutants, we examined cell proliferation and apoptosis, using phospho-histone H3 and cleaved caspase 3 as respective markers. Since *Dlx1* and *Dlx2* are expressed in the mesenchyme but not the epithelium of the palatal region, we focused our analyses on the mesenchyme. At E10.5, we counted mitotic cells in the ventro-medial domain of mxPA1, and also in the ventro-lateral domain for comparison (Fig. 3A). We found that only the ventro-medial area at the posterior level showed a statistically significant decrease in cell proliferation in the mutants (Fig.

3B,C). Similarly, at E11.5, only the posterior palatal shelves showed decrease in cell proliferation in the mutants (Fig. 3D). This result is consistent with the severe growth deficiency in the posterior palate of the mutants.

Although there was a moderate reduction in the size of the mutant palatal shelves at the middle level, we did not find a decrease in mitotic rate at this position at E11.5. We went on to examine cell proliferation at E12.5, and surprisingly, found that the mutant middle palate had higher cell proliferation rate than the controls (Fig. 3E). This result was unique to the middle palate; cell proliferation rates from anterior and posterior levels did not show statistically significant difference between *Dlx1/2*$^{-/-}$ mutants and controls at E12.5 (Fig. 3E). At E13.5, we did not detect significant difference in the cell proliferation rates between the two genotypes at any axial level (Fig. 3F). Increase in cell proliferation in the mutant middle palate at E12.5, although transient, is in apparent contradiction to the decrease in tissue size at the same position found at E13.5. Therefore, more complex mechanisms may underlie the mutant palatal phenotype at the middle level than at the posterior level (see Discussion).

We examined apoptosis in the developing palate at E10.5, E11.5, E12.5 and E13.5, but did not find significant difference between the controls and mutants (data not shown).

Previous studies showed that Cyclin D isoforms are expressed in the palatal shelves and regulate cell proliferation at E13.5 – E14.5 (Ito et al., 2003; Lan and Jiang, 2009; Iwata et al., 2012). We investigated whether expression of these cyclins correlated with the changes in cell proliferation in *Dlx1/2*$^{-/-}$ mutants at E10.5, E11.5 and E12.5 (Fig. 4). For the expression of *Cyclin D1* (*Ccnd1*) and *Cyclin D2* (*Ccnd2*), and other genes discussed later, we are only presenting the pictures for the middle and posterior levels due to space limitations, but we also examined their expression at the anterior level and found no phenotype (data not shown). In the control embryos, both *Ccnd1* and *Ccnd2* were expressed strongly in the mesenchyme of the prospective palate domain at E10.5 (Fig. 4A,C,M,O) and in the newly formed palatal shelves at E11.5 (Fig. 4E,G,Q,S), but at lower levels at E12.5 (I,K,U,W). *Ccnd2* also showed strong expression in the epithelium at all three stages (Fig. 4M,O,Q,S,U,W). In *Dlx1/2*$^{-/-}$ mutants, *Ccnd1* expression was greatly reduced only at the posterior level at both E10.5 and E11.5 (Fig. 4B,D,F,H). At E12.5, *Dlx1/2*$^{-/-}$ middle palate had significantly more *Ccnd1* expression than the control middle palate (Fig. 4I,J). However, in the posterior palate, *Ccnd1* level appeared similar between the two genotypes at this stage (Fig. 4K,L). *Ccnd2* expression in the mutants appeared comparable to that in the controls at all the ages examined (Fig. 4M–X), except for up-regulation in the mesenchyme of the developing upper molar, where ectopic cartilage forms (asterisks in Fig. 4R,V; Thomas et al., 1997). Therefore, the changes in the expression of *Ccnd1*, but not *Ccnd2*, in *Dlx1/2*$^{-/-}$ mutants correlate precisely with the cell proliferation phenotype temporally and spatially.

Decreases in *Ccnd1* expression and cell proliferation in the *Dlx1/2*$^{-/-}$ mutant palate are not caused by a change in Shh signaling

Several studies established that Shh signaling regulates cell proliferation in the palatal mesenchyme around E13.5, either via another signaling molecule Bmp2, or by regulating

Ccnd1 and *Ccnd2* expression (Zhang et al., 2002; Rice et al., 2004; Han et al., 2009; Lan and Jiang, 2009). Therefore, we investigated whether Shh signaling also regulates cell proliferation in the prospective and nascent palate at E10.5 and E11.5. In control embryos, *Shh* was expressed in the epithelium of the palate area at all A-P levels (Fig. 5A,C,E,G; data not shown), and its downstream target gene, *Ptch1*, was expressed in the epithelium and underlying mesenchyme indicating the activation of Hedgehog signaling in these tissues (Fig. 5I,K,M,O; data not shown). To our surprise, we found that the expression of both *Shh* and *Ptch1* was normal in *Dlx1/2*$^{-/-}$ mutants at E10.5, even at the posterior level where *Ccnd1* expression and mitosis were affected (Fig. 5A–D, I–L).

At E11.5, *Shh* and *Ptch1* expression was reduced in the mutants, but the change was mainly at the middle level. In other words, at the posterior level of *Dlx1/2*$^{-/-}$ mutants, cell proliferation was reduced even though Shh signaling appeared quite normal (Fig. 3C,D; Fig. 5K,L,O,P), while at the middle level cell proliferation was not reduced despite severe down-regulation of Shh signaling at E11.5 (Fig. 3D; Fig. 5M,N).

Since *Dlx1* and *Dlx2* are expressed in the mesenchyme but not in the epithelium at the middle level (Fig. 1K,L,Q,R), the change in *Shh* expression in *Dlx1/2*$^{-/-}$ mutants would require intermediary factor(s) relaying the effect from mesenchyme to epithelium. Around E13.5, Bmp4 and Fgf10 are the mesenchymal factors that signal to the epithelium and positively regulate *Shh* expression there (Zhang et al., 2002; Rice et al., 2004). Therefore, we examined the expression of *Fgf10* and *Bmp4* in controls and *Dlx1/2*$^{-/-}$ mutants at E10.5 and E11.5 (Fig. 5Q-f).

Fgf10 is normally expressed in the anterior and middle palate but not the posterior palate at E12.5 – E13.5 (Alappat et al., 2005; Hilliard et al., 2005). This was also true at E10.5 and E11.5 (Fig. 5Q,S,U,W; Alappat et al., 2005). In *Dlx1/2*$^{-/-}$ mutants, *Fgf10* was down-regulated at the middle level at both E10.5 and E11.5 (Fig. 5Q,R,U,V).

Bmp4 is normally expressed only in the anterior palate at E13.5 (Zhang et al., 2002). However, we found its expression in the palatal mesenchyme throughout the A-P axis at E11.5 (Fig. 5c,e); it was not expressed in the future palate area at E10.5 (Fig. 5Y,a). In *Dlx1/2*$^{-/-}$ mutants, *Bmp4* was severely down-regulated in the middle and posterior palate at E11.5 (Fig. 5c–f). Combined, these data suggested that at least at the middle palate, the same mechanism could regulate the epithelial *Shh* expression at E11.5 as at E13.5, namely, through Fgf10 and/or Bmp4 signaling from mesenchyme to epithelium.

Expression of several transcriptional regulators of palatogenesis is affected in *Dlx1/2*$^{-/-}$ palatal shelves

In addition to the signaling molecules, many transcription factors regulate palate development (Gritli-Linde, 2007, 2008; Bush and Jiang, 2012). We found that the expression of five transcription factors with known connection to palatogenesis was lost or greatly reduced in the mxPA1 and palatal shelves of *Dlx1/2*$^{-/-}$ mutants (Fig. 6).

During normal development, a LIM domain-homeodomain transcription factor *Lhx6* (Grigoriou et al., 1998), a homeodomain transcription factor *Barx1* (Tissier-Seta et al.,

1995), a basic helix-loop-helix (bHLH) domain and PERIOD-ARNT-SIM (PAS) domain transcription factor *Sim2* (Dahmane et al., 1995; Fan et al., 1996) and a zinc finger transcription factor *Osr1* (So and Danielian, 1999) are all strongly expressed in PA1 at E10.5 (Fig. 6A,C,E,G) and the nascent palatal shelves at E11.5 (Fig. 6I,K,M,O,Q,S,U,W). Another zinc finger transcription factor, *Osr2*, is expressed in small domains of PA1 at E10.5 but is rapidly up-regulated in the palatal shelves one day later (Fig. 6Y,a; Lan et al., 2004). In *Dlx1/2*$^{-/-}$ mutants, the expression of all five genes was severely down-regulated in mxPA1 and the palatal shelves (Fig. 6A-b).

Mouse mutants for *Barx1* and *Sim2* have cleft palate defect (Shamblott et al., 2002; Kim et al., 2007; Miletich et al., 2011); while the details on the palate phenotype of *Barx1* mutants have yet to be reported, in *Sim2* mutants the defect was apparent first at E14.5 as reduced cell density in the mesenchyme and later as smaller palatal shelves (Shamblott et al., 2002). *Lhx6* has been implicated in palatogenesis because mice missing the activities of its homolog *Lhx8* (also known as *Lhx7*) (*Lhx8*$^{-/-}$) or both *Lhx6* and *Lhx8* (*Lhx6*$^{-/-}$;*Lhx8*$^{-/-}$) have cleft palate (Zhao et al., 1999; Denaxa et al., 2009). We found that *Lhx6* single mutants (*Lhx6*$^{-/-}$) had a fused palate, but skeleton preparations revealed that they had no or very small palatal processes of maxilla (Fig. 6c,d; N=5). Direct evidence for the importance of *Osr1* in palatogenesis has not been reported. On the other hand, *Osr2* was shown to be essential for normal growth of the palatal shelves from E13.5 (Lan et al., 2004).

Analysis of *Dlx2*$^{-/-}$ mutant palate phenotype

Inactivating *Dlx2* alone is sufficient to cause cleft palate, although with incomplete penetrance (80%; Qiu et al., 1995). Morphological examination at E13.5 revealed growth deficiency in the palatal shelves of *Dlx2*$^{-/-}$ (Fig. 7A–D), but it was much milder than what was observed in *Dlx1/2*$^{-/-}$ mutants. Neither *Ccnd1* expression (at E10.5 and E11.5) nor cell proliferation rate (at E11.5) appeared significantly different between *Dlx2*$^{-/-}$ mutant and control palate areas (Fig. 7E–I), although we cannot rule out the possibility that subtle changes below the sensitivity limit of our methods may underlie the palate hypoplasia of *Dlx2*$^{-/-}$ mutants.

We examined whether the expression of the genes that were down-regulated in *Dlx1/2*$^{-/-}$ mutants was also affected in *Dlx2*$^{-/-}$ mutants. *Shh* and *Ptch1* were down-regulated at the medial edge of the middle palate but appeared normal in the posterior palate (Fig. 7J–Q). *Fgf10* expression did not appear altered in *Dlx2*$^{-/-}$ mutant (Fig. 7R,S), but *Bmp4* expression was clearly down-regulated (Fig. 7T–W). As for the transcription factor genes, expression of *Lhx6*, *Barx1* and *Osr2* was moderately reduced in *Dlx2*$^{-/-}$ mutants (Fig. 7X-a, f–i), whereas *Sim2* and *Osr1* expression was greatly reduced in *Dlx2*$^{-/-}$ mxPA1 (Fig. 7b–e). Therefore, the changes in the expression of *Shh*, *Ptch1*, *Bmp4*, *Lhx6*, *Barx1*, *Sim2*, *Osr1* and *Osr2* may contribute to the cleft palate phenotype of *Dlx2*$^{-/-}$ mutants.

Discussion

Role of *Dlx1/2* in early palate development

In this study, we investigated the etiology of the cleft palate of mouse *Dlx1/2*$^{-/-}$ mutants. We provide evidence that *Dlx1* and *Dlx2* regulate the initiation of palatogenesis through promoting mesenchymal proliferation in the posterior palate independently of Shh signaling. The early growth defect in *Dlx1/2*$^{-/-}$ mutants was highly localized to the posterior palate, indicating the existence of heterogeniety along the A-P axis as found at later stages of development (Hillard et al., 2005; Yu and Ornitz, 2011). Decreases in *Ccnd1* expression and cell proliferation rate provided molecular and cellular explanations for the growth phenotype in the posterior palate. In addition, our evidence suggests that *Dlx1* and *Dlx2* non-autonomously promote *Shh* epithelial expression through Bmp4 and Fgf10 in the middle palate, and further regulate palatal development through promoting mesenchymal expression of the *Lhx6*, *Barx1*, *Sim2*, *Osr1* and *Osr2* transcription factors.

One confounding result from our analysis of palate development was that, at least at one point (E12.5), *Dlx1/2*$^{-/-}$ mutants had a higher cell proliferation rate than the controls in the middle palate (Fig. 3), even though the mutant middle palate was consistently smaller than the controls (Fig. 2). While increase in cell death could counter the effect of increase in cell proliferation, we did not find a significant difference in apoptosis rates between the control and mutant palate at E10.5 – E13.5 (data not shown). Another possibility is that cell distribution is somehow altered in the mutant middle palate; for example, cells generated at the middle palate might migrate or be displaced posteriorly, where they would partially fill the void that would otherwise be left in the posterior half of the oral cavity. Cells from the mutant middle palate might also have been shifted toward dorso-lateral region of the upper jaw, another region that has a growth deficiency (Fig. 2). If more cells “leave” the middle palate through such redistribution than those produced by enhanced cell proliferation in that region, then the net effect would be the decrease in the size of the middle palate.

Timing of *Dlx1/2* action

Two studies from other species suggested that *Dlx2* plays important roles in the pre-migratory and/or migrating cranial neural crest cells (CNCCs) before their arrival at the PAs; knockdown of *dlx2a* expression in zebra fish caused increased apoptosis in migrating CNCCs (Sperber et al., 2008). In addition, ectopic expression of *Dlx2* in the premigratory CNCCs of chick embryos inhibited migration of these cells (McKeown et al., 2005). This raises the question of whether the palate defect of mouse *Dlx1/2*$^{-/-}$ mutants is an indirect consequence of the abnormalities in the pre-migratory/migrating CNCC population. We do not believe this is the case due to the following reasons. First, neither *Dlx1* nor *Dlx2* is expressed in the pre-migratory CNCCs in mice (Fig. 1; Dollé et al., 1992; Bulfone et al., 1993; Robinson and Mahon, 1994). While *Dlx2* is expressed in the migrating CNCCs (Fig. 1; Bulfone et al., 1993; Robinson and Mahon, 1994), we did not find any difference between *Dlx1/2*$^{-/-}$ mutants and controls in the expression patterns of a gene that marks migrating CNCCs, namely, *Tcfap2a* (Mitchell et al., 1991) (Fig. 8A,B), apoptosis of the migrating cells (Fig. 8C,D), nor the contribution of CNCCs to the PA1 mesenchyme labeled by Wnt1-Cre reporter system (Fig. 8E,F; Danielian et al., 1998; Soriano, 1999; Chai et al., 2000).

Therefore, there is no indication that the migration of CNCCs to PA1 was affected in *Dlx1/2*$^{-/-}$ mutants. The second line of evidence comes from the fact that the cleft palate phenotype of *Dlx1/2*$^{-/-}$ mutants is much more severe than that of *Dlx2*$^{-/-}$ mutants (compare Figs. 2 and 7); this indicates that in *Dlx2*$^{-/-}$ single mutants, *Dlx1* performs some of the normal functions of *Dlx2* that are important for palate development. Since *Dlx1* is not expressed in the migrating CNCCs (Fig. 8G,H) but is co-expressed with *Dlx2* in the post-migratory CNCCs in PA1 (Fig. 1; Dollé et al., 1992; Bulfone et al., 1993; Robinson and Mahon, 1994), the parsimonious explanation is that the actions of *Dlx1* and *Dlx2* that are important to palatogenesis occur at PA1, and not in the migrating CNCCs. The same logic applies to most other craniofacial defects of *Dlx1/2*$^{-/-}$ because they are more severe than those of *Dlx2*$^{-/-}$ (Qiu et al., 1995, 1997). Therefore, we conclude that in mice, the timing for the major functions of *Dlx1* and *Dlx2* in the craniofacial development is after CNCCs reach PA1.

Genetic regulation of the initiation of palatogenesis

Despite the recent progress in our understanding of the palate development, what regulates the initiation of palatogenesis is largely unknown. This can be attributed to the fact that in almost all the mouse mutants reported to have cleft palate, the initial formation of the palatal shelves and the early part of the vertical growth (up to E12.5) were unaffected, and defects appeared only in the mid- to late-stages of palatogenesis (E13 and later) (Gritli-Linde, 2007, 2008; Bush and Jiang, 2012). Prior to the current study, there have been only a couple of examples where the inactivation of a gene led to hypoplasia of developing upper jaw before E12.5 that was not caused by problems in CNCC production or migration. Embryos with neural crest-specific inactivation of *Alk5* (encoding TGFβ type I receptor) or *Smad4* (encoding a transcriptional regulator downstream of TGFβ) had hypoplastic mxPA1 from E10.5 – E11 (Dudas et al., 2006; Ko et al, 2007). However, in both cases, it was the increase in cell death, not a change in proliferation, which caused the hypoplasia. By contrast, region-specific reduction in cell proliferation was behind the growth deficiency of posterior palatal shelves in *Dlx1/2*$^{-/-}$ mutants, which was evident by E11.5. Therefore, *Dlx1/2*$^{-/-}$ mutants present a unique example where the initial formation of the palatal shelves is disrupted and the phenotype cannot simply be explained by general compromise in tissue integrity.

Signaling pathways regulating cell proliferation in the palate

How cell proliferation is regulated in the developing palate is best understood around E13.5, shortly before the palatal shelves change orientation from vertical to horizontal. *Shh* expression in the epithelium has a central role at this stage; Bmp4, Fgf10 and Fgf7 produced in the palatal mesenchyme signal to the epithelium, where Bmp4 and Fgf10 positively regulate *Shh* expression, whereas Fgf7 represses *Shh* expression (Zhang et al., 2002; Rice et al., 2004; Han et al., 2009). Shh then signals back to the mesenchyme to promote proliferation, either via Bmp2 or by directly regulating *Ccnd1* and *Ccnd2*, depending on the position along the A-P axis (Zhang et al., 2002; Lan and Jiang, 2009).

A recent study identified another genetic pathway crucial for cell proliferation in the palate, operating after palatal shelf elevation (E14.5) (Iwata et al., 2012); at this time, Fgf9 is the

mitogen positively regulating *Ccnd1* and *Ccnd3* expression. *Fgf9* expression is regulated by TGFβ signaling.

At E10.5 – E11.5, when we found reduced cell proliferation in *Dlx1/2*$^{-/-}$ mutants, *Shh* is expressed in the epithelium of the ventro-medial quadrant of mxPA1, the location of palatal shelf outgrowth (Fig. 5; Jeong et al., 2004). On the other hand, *Fgf9* is expressed more laterally at the dental lamina (Kettunen and Thesleff, 1998; Colvin et al., 1999). However, despite *Shh* being expressed at the right place and time, it did not mediate the decrease in cell proliferation in the posterior palate of *Dlx1/2*$^{-/-}$ mutants. Conversely, removing Shh signaling in mxPA1 mesenchyme did not affect the expression of *Dlx1* and *Dlx2* here, indicating that the *Dlx* genes are not downstream of Shh signaling (Jeong et al., 2004). Therefore, the regulation of cell proliferation by *Dlx1* and *Dlx2* at the beginning of palatogenesis (E10.5 – E11.5) is through a mechanism independent of Shh, the details of which remain to be elucidated.

Effect of *Dlx1/2* on later stages of palate development

In addition to the early growth defect, the developing palate of *Dlx1/2*$^{-/-}$ mutants exhibited changes in the expression of several genes implicated in palate development; expression of *Shh, Fgf10* and *Bmp4*, which form a signaling loop important for cell proliferation around E13.5 (Zhang et al., 2002; Rice et al., 2004; Lan and Jiang, 2009), was down-regulated at the middle palate of *Dlx1/2*$^{-/-}$ mutants by E11.5 (Fig. 5). Also, the expression of *Lhx6, Barx1, Sim2, Osr1* and *Osr2* was lost or greatly reduced at E10.5 and E11.5 (Fig. 6). Therefore, although the severe early defect in *Dlx1/2*$^{-/-}$ mutants masks any perturbation of the later steps of palatogenesis, *Dlx1* and *Dlx2* likely play indirect but extensive roles as upstream regulators of other important factors for this process.

Experimental Procedures

Animals

All the experiments using mice were performed following protocols approved by UCSF, NICHD or NYU institutional committee on the use of laboratory animals. Mice carrying targeted mutant alleles of *Dlx2, Dlx1/2* and *Lhx6* have been previously described (Qiu et al., 1995, 1997; Choi et al., 2005). For all the mutant lines used in this study, the animals were of mixed genetic background of 129, C57Bl/6 and CD1. As controls for the homozygote mutants (−/−), littermate heterozygote (+/−) or wild type (+/+) embryos were used without distinction. For each experiment, mutant and control embryos were carefully stage-matched; at E8.5 – E11.5, we used the number of somites as a criterion. At E12.5 and beyond, we used a combination of morphological criteria including overall size of the body, size and shape of the limb buds and degree of digitation.

Preparation of sections

All the tissue sections used in this study are frozen sections. Embryos were dissected in phosphate-buffered saline (PBS), fixed in 4% paraformaldehyde at 4°C for 1–2 days, incubated in 10% and then 20% sucrose in PBS for cryoprotection, and embedded in OCT compound (Tissue-Tek) for coronal sections. Sections were cut at 12 μm (E10.5) – 18 μm

(E14.5), and collected on slides such that each slide contains the sections covering the entire antero-posterior (A-P) length of the oral cavity at a 48 μm (E10.5) – 180 μm (E14.5) interval. Therefore, for each section in situ hybridization or immunofluorescence experiment presented in this paper, we examined the marker expression in the whole sets of sections and drew conclusions, even though no more than three sections (representing anterior, middle and posterior levels) per genotype are shown in the figures. To select anterior, middle and posterior sections of the palatal region consistently across different genotypes and ages, we used the following criteria; “anterior” is just anterior to the upper molars. “Middle” is from the level of upper molars to the level of lower molars, and included eyes and optic stalks/nerves in the section. “Posterior” is just posterior to the molars and eyes.

In situ hybridization, cresyl violet staining, skeleton preparation and cell death assays

Whole mount and section in situ hybridizations were performed using digoxigenin-labeled RNA probes as previously described (Jeong et al., 2004, 2008). DNA templates for in situ hybridization probes were obtained from other researchers, purchased from companies, or PCR-cloned from mouse E10.5 PA1 cDNA library or tail genomic DNA. Further information on the probes is available upon request. To visualize tissue morphology, the sections were stained with 0.1% cresyl violet solution for 10 minutes, washed and dehydrated with ethanol and xylene, and coversliped with Permount (Fisher). Skeleton staining of new-born animals was performed as previously described (Jeong et al., 2004). Cell death was detected on tissue sections using anti-cleaved caspase3 antibody (Cell Signaling Technology) or in whole embryos using LysoTracker (Invitrogen) as previously described (Jeong et al., 2004; Grieshammer et al., 2005).

Quantitative analyses of the size of the palatal shelves, cell proliferation rates and cell density

The areas of the (prospective) palatal shelves were measured from sections stained with DAPI (E11.5) or cresyl violet (E13.5) using ImageJ program (Abramoff et al., 2004). The boundary of a palatal shelf was defined as marked in Figure 2. Three control and three mutant embryos were analyzed at each stage, and from each embryo two palatal shelves were measured. Student’s T-test was used to determine if the differences between the genotypes were statistically significant.

Immunofluorescence for phospho-histone H3 was performed as previously described (Jeong et al., 2004) using an antibody from Upstate Biochem and DAPI for nuclear counter staining. To calculate the percentage of mitotic cells, we first counted total number of cells in a defined area from DAPI staining, by automated counting using ImageJ plug-in followed by manual confirmation. Then the number of phospho-histone H3-positive cells from the same area was counted manually, and this number was divided by the total number of cells. At E10.5, there are yet no palatal shelves that one can demarcate, and thus we defined prospective palate area as the medial half of the ventral mxPA1, whose dorsal boundary was a straight line at a fixed distance from the mid-point of the ventral epithelium of mxPA1 (see Fig. 3A). The medial boundary of mxPA1 was matched among different samples using stereotypical bendings of the ventral epithelium as landmarks. At E11.5 and E12.5, the countings were performed in the palatal shelves as demarcated in Figure 2. For each stage,

three embryos per genotype, two (prospective) palatal shelves per embryo were analyzed, and Student's T-test was used to determine if the differences between the genotypes were statistically significant.

To determine the mesenchymal cell density in the posterior palate at E10.5, we measured the area of the posterior palate (boundaries defined as described above) from DAPI-stained sections using ImageJ, and then used this value to divide the total number of cells in that area (which was counted as described above). Three embryos per genotype, two prospective palatal shelves per embryo were analyzed, and Student's T-test was used to determine if the difference between the genotypes was statistically significant.

Acknowledgments

We thank Regeneron for *Lhx6* mutant mice (MAID#406), Purvi Patel for genotyping mice and embryos, Hideyo Ohuchi, Joy Yang and Jun Aruga for in situ hybridization probes, Jason Long, Jeremy Cholfin, Inma Cobos, Greg Potter and Andrea Faedo for sharing reagents and ideas, and Gail Martin, Ophir Klein, Ross Metzger, Maria Barna and the members of Rubenstein lab and Martin lab for helpful discussions. This work was funded by grants from NIH (NIDCD R01 DC05667), March of Dimes, Weston Havens Foundation, Hillblom Foundation and Nina Ireland to J.L.R.R., by a grant from NIH (NIDCR K99/R00 DE019486) to J.J. and by funds from the NICHD intramural research program to H.W.

References

Abramoff MD, Magalhaes PJ, Ram SJ. Image Processing with ImageJ. Biophotonics Intl. 2004; 11:36–42.

Acampora D, Merlo GR, Paleari L, Zerega B, Pia Postiglione M, Mantero S, Bober E, Barbieri O, Simeone A, Levi G. Craniofacial, vestibular and bone defects in mice lacking the Distal-less related gene Dlx5. Development. 1999; 126:3795–3809. [PubMed: 10433909]

Alappat SR, Zhang Z, Suzuki K, Zhang X, Liu H, Jiang R, Yamada G, Chen Y. The cellular and molecular etiology of the cleft secondary palate in Fgf10 mutant mice. Dev Biol. 2005; 277:102–113. [PubMed: 15572143]

Anderson S, Eisenstat D, Shi L, Rubenstein JL. Interneuron migration from basal forebrain to neocortex: dependence on Dlx genes. Science. 1997; 278:474–476. [PubMed: 9334308]

Beverdam A, Merlo GR, Paleari L, Mantero S, Genova F, Barbieri O, Janvier P, Levi G. Jaw transformation with gain of symmetry after Dlx5/Dlx6 inactivation: mirror of the past? Genesis. 2002; 34:221–227. [PubMed: 12434331]

Bulfone A, Kim HJ, Puelles L, Porteus MH, Grippo JF, Rubenstein JL. The mouse Dlx-2 (Tes-1) gene is expressed in spatially restricted domains of the forebrain, face and limbs in midgestation mouse embryos. Mech Dev. 1993; 40:129–140. [PubMed: 8098616]

Bush JO, Jiang R. Palatogenesis: morphogenetic and molecular mechanisms of secondary palate development. Development. 2012; 139:231–243. [PubMed: 22186724]

Chai Y, Jiang X, Ito Y, Bringas P Jr, Han J, Rowitch DH, Soriano P, McMahon AP, Sucov HM. Fate of the mammalian cranial neural crest during tooth and mandibular morphogenesis. Development. 2000; 127:1671–1679. [PubMed: 10725243]

Choi GB, Dong HW, Murphy AJ, Valenzuela DM, Yancopoulos GD, Swanson LW, Anderson DJ. Lhx6 delineates a pathway mediating innate reproductive behaviors from the amygdala to the hypothalamus. Neuron. 2005; 46:647–660. [PubMed: 15944132]

Colvin JS, Feldman B, Nadeau JH, Goldfarbm M, Ornitz DM. Genomic organization and embryonic expression of the mouse fibroblast growth factor 9 gene. Dev Dyn. 1999; 216:72–88. [PubMed: 10474167]

Dahmane N, Charron G, Lopes C, Yaspo ML, Maunoury C, Decorte L, Sinet PM, Bloch B, Delabar JM. Down syndrome-critical region contains a gene homologous to Drosophila sim expressed

during rat and human central nervous system development. Proc Natl Acad Sci USA. 1995; 92:9191–9195. [PubMed: 7568099]

Danielian PS, Muccino D, Rowitch DH, Michael SK, McMahon AP. Modification of gene activity in mouse embryos in utero by a tamoxifen-inducible form of Cre recombinase. Curr Biol. 1998; 8:1323–1326. [PubMed: 9843687]

Denaxa M, Sharpe PT, Pachnis V. The LIM homeodomain transcription factors Lhx6 and Lhx7 are key regulators of mammalian dentition. Dev Biol. 2009; 333:324–336. [PubMed: 19591819]

Depew MJ, Liu JK, Long JE, Presley R, Meneses JJ, Pedersen RA, Rubenstein JLR. Dlx5 regulates regional development of the branchial arches and sensory capsules. Development. 1999; 126:831–3846.

Depew MJ, Lufkin T, Rubenstein JLR. Specification of jaw subdivisions by Dlx genes. Science. 2002; 298:381–385. [PubMed: 12193642]

Dixon MJ, Marazita ML, Beaty TH, Murray JC. Cleft lip and palate: understanding genetic and environmental influences. Nat Rev Genet. 2011; 12:167–178. [PubMed: 21331089]

Dollé P, Price M, Duboule D. Expression of the murine Dlx-1 homeobox gene during facial, ocular and limb development. Differentiation. 1992; 49:93–99. [PubMed: 1350766]

Dudas M, Kim J, Li W-Y, Nagy A, Larsson J, Karlsson S, Chai Y, Kaartinen V. Epithelial and ectomesenchymal role of the type I TGF-β receptor ALK5 during facial morphogenesis and palatal fusion. Dev Biol. 2006; 296:298–314. [PubMed: 16806156]

Fan CM, Kuwana E, Bulfone A, Fletcher CF, Copeland NG, Jenkins NA, Crews S, Martinez S, Puelles L, Rubenstein JL, Tessier-Lavigne M. Expression patterns of two murine homologs of Drosophila single-minded suggest possible roles in embryonic patterning and in the pathogenesis of Down syndrome. Mol Cell Neurosci. 1996; 7:1–16. [PubMed: 8812055]

Ferguson MW. Palate development. Development. 1988; 103(Suppl):41–60. [PubMed: 3074914]

Grieshammer U, Cebrián C, Ilagan R, Meyers E, Herzlinger D, Martin GR. FGF8 is required for cell survival at distinct stages of nephrogenesis and for regulation of gene expression in nascent nephrons. Development. 2005; 132:3847–3857. [PubMed: 16049112]

Grigoriou M, Tucker AS, Sharpe PT, Pachnis V. Expression and regulation of Lhx6 and Lhx7, a novel subfamily of LIM homeodomain encoding genes, suggests a role in mammalian head development. Development. 1998; 125:2063–2074. [PubMed: 9570771]

Gritli-Linde A. Molecular control of secondary palate development. Dev Biol. 2007; 301:309–326. [PubMed: 16942766]

Gritli-Linde A. The etiopathogenesis of cleft lip and cleft palate: usefulness and caveats of mouse models. Curr Top Dev Biol. 2008; 84:37–138. [PubMed: 19186243]

Han J, Mayo J, Xu X, Li J, Bringas P Jr, Maas RL, Rubenstein JLR, Chai Y. Indirect modulation of Shh signaling by Dlx5 affects the oral-nasal patterning of palate and rescues cleft palate in Msx1-null mice. Development. 2009; 136:4225–4233. [PubMed: 19934017]

Hilliard SA, Yu L, Gu S, Zhang Z, Chen YP. Regional regulation of palatal growth and patterning along the anterior-posterior axis in mice. J Anat. 2005; 207:655–667. [PubMed: 16313398]

Ito Y, Yeo JY, Chytil A, Han J, Bringas P Jr, Nakajima A, Shuler CF, Moses HL, Chai Y. Conditional inactivation of Tgfbr2 in cranial neural crest causes cleft palate and calvaria defects. Development. 2003; 130:5269–5280. [PubMed: 12975342]

Iwata J, Tung L, Urata M, Hacia JG, Pelikan R, Suzuki A, Ramenzoni L, Chaudhry O, Parada C, Sanchez-Lara P, Chai Y. Fibroblast growth factor 9 (Fgf9)-Pituitary homeobox 2 (Pitx2) pathway mediates transforming growth factor β (Tgfβ) signaling to regulate cell proliferation in palatal mesenchyme during mouse palatogenesis. J Biol Chem. 2012; 287:2353–2363. [PubMed: 22123828]

Jeong J, Mao J, Tenzen T, Kottmann AH, McMahon AP. Hedgehog signaling in the neural crest cells regulates the patterning and growth of facial primordia. Genes Dev. 2004; 18:937–951. [PubMed: 15107405]

Jeong J, Li X, McEvilly R, Rosenfeld MG, Lufkin T, Rubenstein JLR. Dlx genes pattern mammalian jaw primordium by regulating both lower jaw-specific and upper jaw-specific genetic programs. Development. 2008; 135:2905–2916. [PubMed: 18697905]

Kettunen P, Thesleff I. Expression and function of FGFs-4, -8, and -9 suggest functional redundancy and repetitive use as epithelial signals during tooth morphogenesis. Dev Dyn. 1998; 211:256–268. [PubMed: 9520113]

Kim BM, Miletich I, Mao J, McMahon AP, Sharpe PA, Shivdasani RA. Independent functions and mechanisms for homeobox gene Barx1 in patterning mouse stomach and spleen. Development. 2007; 134:3603–3613. [PubMed: 17855428]

Ko SO, Chung IH, Xu X, Oka S, Zhao H, Cho ES, Deng C, Chai Y. Smad4 is required to regulate the fate of cranial neural crest cells. Dev Biol. 2007; 312:435–447. [PubMed: 17964566]

Lan Y, Jiang R. Sonic hedgehog signaling regulates reciprocal epithelial-mesenchymal interactions controlling palatal outgrowth. Development. 2009; 136:1387–1396. [PubMed: 19304890]

Lan Y, Ovitt CE, Cho ES, Maltby KM, Wang Q, Jiang R. Odd-skipped related 2 (Osr2) encodes a key intrinsic regulator of secondary palate growth and morphogenesis. Development. 2004; 131:3207–3216. [PubMed: 15175245]

McKeown SJ, Newgreen DF, Farlie PG. Dlx2 over-expression regulates cell adhesion and mesenchymal condensation in ectomesenchyme. Dev Biol. 2005; 281:22–37. [PubMed: 15848386]

Merlo GR, Paleari L, Mantero S, Zerega B, Adamska M, Rinkwitz S, Bober E, Levi G. The Dlx5 homeobox gene is essential for vestibular morphogenesis in the mouse embryo through a BMP4-mediated pathway. Dev Biol. 2002; 248:157–169. [PubMed: 12142028]

Miletich I, Yu WY, Zhang R, Yang K, Caixeta de Andrade S, Pereira SF, Ohazama A, Mock OB, Buchner G, Sealby J, Webster Z, Zhao M, Bei M, Sharpe PT. Developmental stalling and organ-autonomous regulation of morphogenesis. Proc Natl Acad Sci USA. 2011; 108:19270–19275. [PubMed: 22084104]

Mitchell PJ, Timmons PM, Hebert JM, Rigby PWJ, Tjian R. Transcription factor AP-2 is expressed in neural crest cell lineages during mouse embryogenesis. Genes dev. 1991; 5:105–119. [PubMed: 1989904]

Panganiban G, Rubenstein JLR. Developmental functions of the Distal-less/Dlx homeobox genes. Development. 2002; 129:4371–4836. [PubMed: 12223397]

Porteus MH, Bulfone A, Ciaranello RD, Rubenstein JLR. Isolation and characterization of a novel cDNA clone encoding a homeodomain that is developmentally regulated in the ventral forebrain. Neuron. 1991; 77:221–229. [PubMed: 1678612]

Price M, Lemaistre M, Pischetola M, di Lauro R, Duboule D. A mouse gene related to Distal-less shows a restricted expression in the developing forebrain. Nature. 1991; 351:748–751. [PubMed: 1676488]

Qiu M, Bulfone A, Martinez S, Meneses J, Shimamura K, Pedersen RA, Rubenstein JLR. Null mutation of Dlx-2 results in abnormal morphogenesis of proximal first and second branchial arch derivatives and abnormal differentiation in the forebrain. Genes Dev. 1995; 9:2523–2538. [PubMed: 7590232]

Qiu M, Bulfone A, Ghattas I, Meneses JJ, Christensen L, Sharpe PT, Presley R, Pederson RA, Rubenstein JLR. Role of the Dlx homeobox genes in proximodistal patterning of the branchial arches: mutations of Dlx-1, Dlx-2, and Dlx-1 and-2 alter morphogenesis of proximal skeletal and soft tissue structures derived from the first and second arches. Dev Biol. 1997; 185:165–184. [PubMed: 9187081]

Rice R, Spencer-Dene B, Connor EC, Gritli-Linde A, McMahon AP, Dickson C, Thesleff I, Rice DP. Disruption of Fgf10/Fgfr2b-coordinated epithelial-mesenchymal interactions causes cleft palate. J Clin Invest. 2004; 113:1692–1700. [PubMed: 15199404]

Robinson GW, Mahon KA. Differential and overlapping expression domains of Dlx-2 and Dlx-3 suggest distinct roles for Distal-less homeobox genes in craniofacial development. Mech Dev. 1994; 48:199–215. [PubMed: 7893603]

Robledo RF, Lufkin T. Dlx5 and Dlx6 homeobox genes are required for specification of the mammalian vestibular apparatus. Genesis. 2006; 44:425–437. [PubMed: 16900517]

Robledo RF, Rajan L, Li X, Lufkin T. The Dlx5 and Dlx6 homeobox genes are essential for craniofacial, axial, and appendicular skeletal development. Genes Dev. 2002; 16:1089–1101. [PubMed: 12000792]

Shamblott MJ, Bugg EM, Lawler AM, Gearhart JD. Craniofacial abnormalities resulting from targeted disruption of the murine Sim2 gene. Dev Dyn. 2002; 224:373–380. [PubMed: 12203729]

Simeone A, Acampora D, Pannese M, D'Esposito M, Stornaiuolo A, Gulisano M, Mallamaci A, Kastury K, Druck T, Huebner K, Boncinelli E. Cloning and characterization of two members of the vertebrate Dlx gene family. Proc Natl Acad Sci USA. 1994; 91:2250–2254. [PubMed: 7907794]

So PL, Danielian PS. Cloning and expression analysis of a mouse gene related to Drosophila odd-skipped. Mech Dev. 1999; 84:157–160. [PubMed: 10473132]

Soriano P. Generalized LacZ expression with the ROSA26 Cre reporter strain. Nat Genet. 1999; 21:70–71. [PubMed: 9916792]

Sperber SM, Saxena V, Hatch G, Ekker M. Zebrafish dlx2a contributes to hindbrain neural crest survival, is necessary for differentiation of sensory ganglia and functions with dlx1a in maturation of the arch cartilage elements. Dev Biol. 2008; 314:59–70. [PubMed: 18158147]

Thomas BL, Tucker AS, Qui M, Ferguson CA, Hardcastle Z, Rubenstein JL, Sharpe PT. Role of Dlx-1 and Dlx-2 genes in patterning of the murine dentition. Development. 1997; 124:4811–4818. [PubMed: 9428417]

Tissier-Seta JP, Mucchielli ML, Mark M, Mattei MG, Goridis C, Brunet JF. Barx1, a new mouse homeodomain transcription factor expressed in cranio-facial ectomesenchyme and the stomach. Mech Dev. 1995; 51:3–15. [PubMed: 7669690]

Tolarova MM, Cervenka J. Classification and birth prevalence of orofacial clefts. Am J Med Genet. 1998; 75:126–137. [PubMed: 9450872]

Yu K, Ornitz DM. Histomorphological study of palatal shelf elevation during murine secondary palate formation. Dev Dyn. 2011; 240:1737–1744. [PubMed: 21618642]

Zhang Z, Song Y, Zhao X, Zhang X, Fermin C, Chen Y. Rescue of cleft palate in Msx1-deficient mice by transgenic Bmp4 reveals a network of BMP and Shh signaling in the regulation of mammalian palatogenesis. Development. 2002; 129:4135–4146. [PubMed: 12163415]

Zhao Y, Guo YJ, Tomac AC, Taylor NR, Grinberg A, Lee EJ, Huang S, Westphal H. Isolated cleft palate in mice with a targeted mutation of the LIM homeobox gene lhx8. Proc Natl Acad Sci USA. 1999; 96:15002–15006. [PubMed: 10611327]

Bullet points

- We investigated the etiology underlying cleft palate of mouse *Dlx1/2*$^{-/-}$ mutants.
- The posterior palate failed to grow in these mutants from the onset of palatogenesis.
- Cell proliferation rate and Cyclin D1 expression were reduced in the mutant posterior palate.
- Expression of multiple known regulators of palatogenesis was affected in the mutants.
- We conclude that *Dlx1* and *Dlx2* are crucial for early stages of palatogenesis.

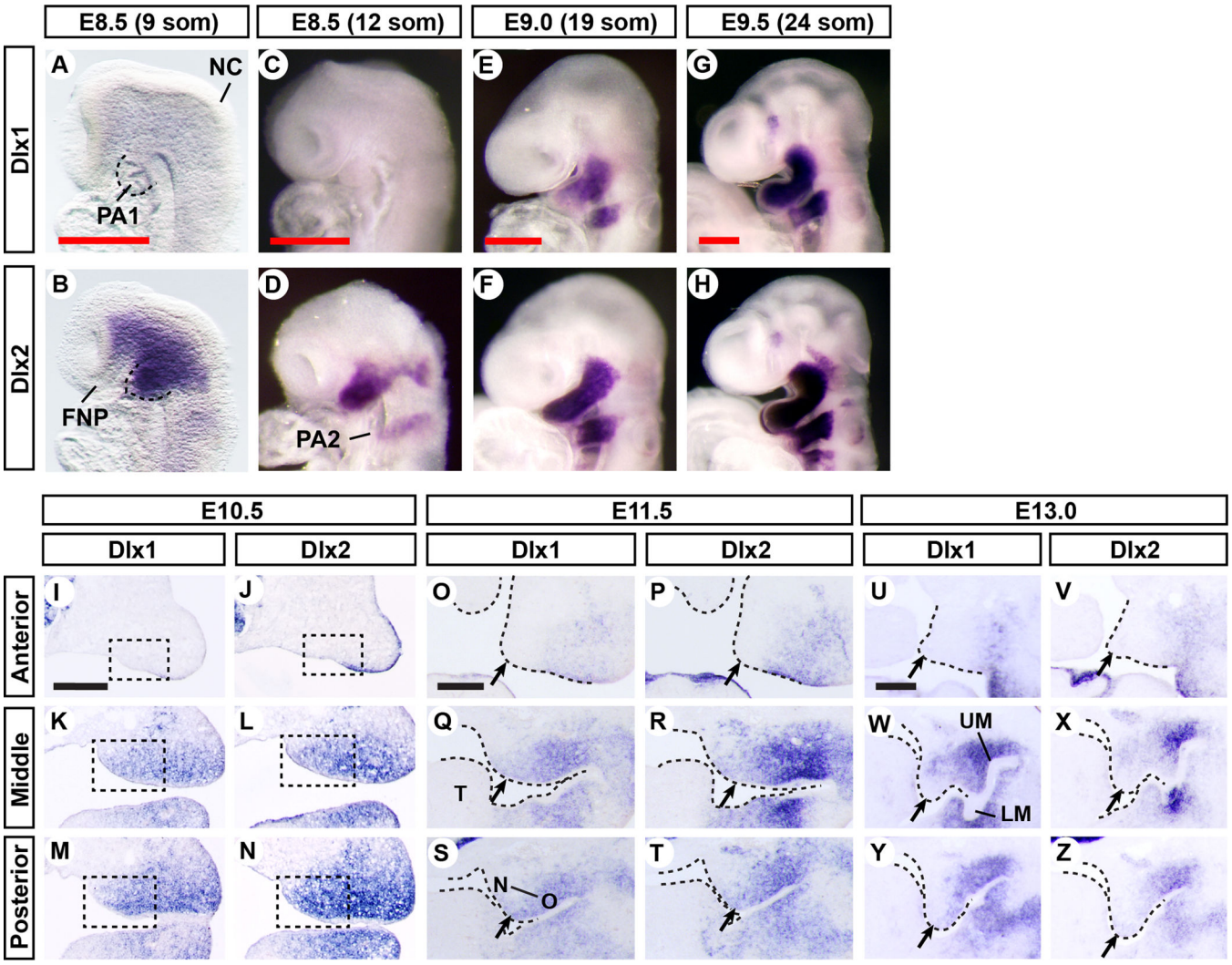

Figure 1. Expression patterns of *Dlx1* and *Dlx2* during normal development

(A–H) Lateral views of the heads of wild type embryos processed by whole mount in situ hybridization. The probes and stages of the embryos are as indicated in the figure. The stages are shown both in embryonic days and in somite numbers. (I–Z) Coronal sections of the orofacial region of wild type embryos processed by section in situ hybridization. Only the right half of the face is shown. The probes and stages of the embryos are as indicated in the figure. The boxes in I–N indicate prospective palate domains within mxPA1. The arrows in O–Z point to the palatal shelves. Nasal (N) – Oral (O) axis of the palatal shelf is indicated on S. Abbreviations: FNP, frontonasal prominence; LM, lower molar; NC, neural crest; PA1, first pharyngeal arch; PA2, second pharyngeal arch; T, tongue; UM, upper molar. Bar, 0.25 mm.

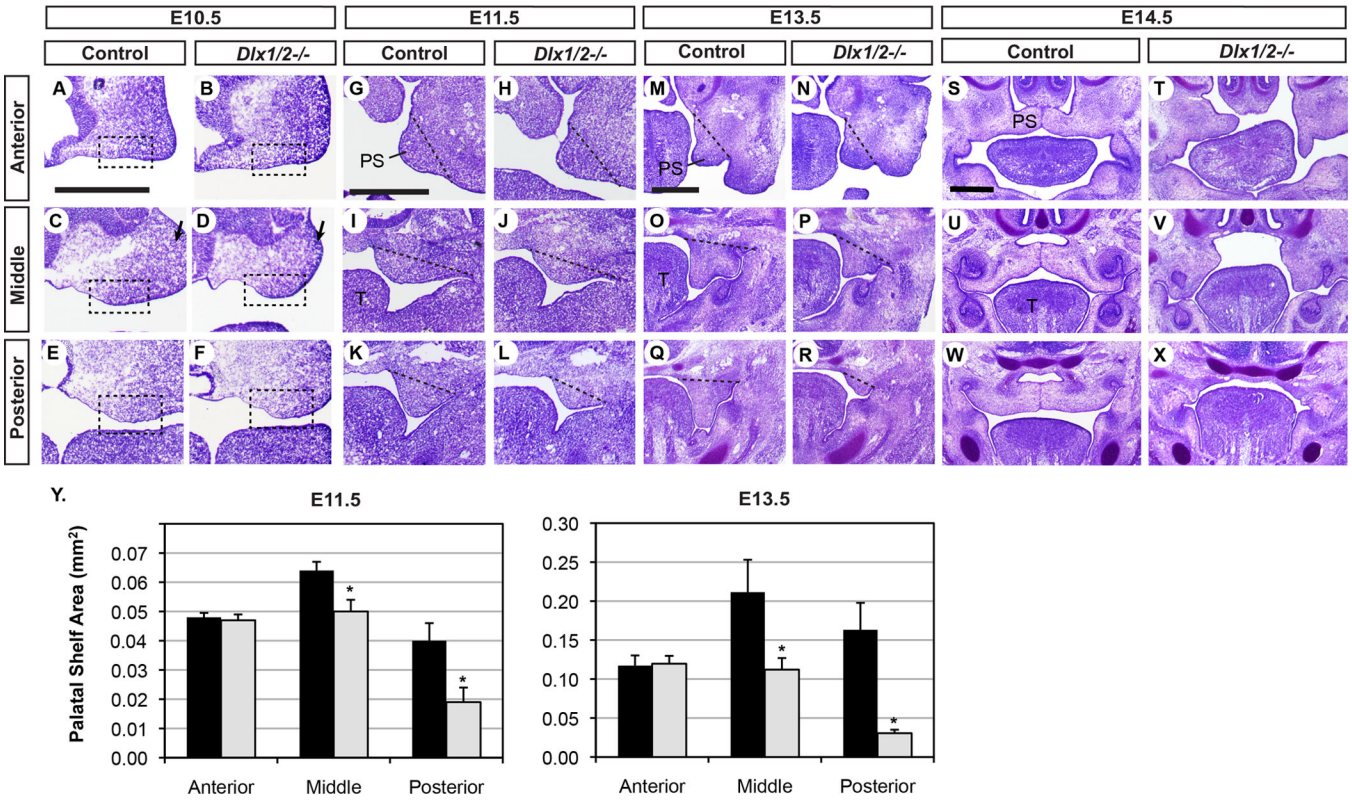

Figure 2. Morphological analysis of the developing palate of *Dlx1/2*$^{-/-}$ mutants

(A–X) Coronal sections of the orofacial region of control and *Dlx1/2*$^{-/-}$ mutant embryos stained with cresyl violet. The stages of the embryos are as indicated in the figure. The boxes in A–F indicate prospective palate domains within mxPA1. The arrows in C and D point out the hypoplasia of dorso-lateral mxPA1 in the mutant. The dotted lines in G–R indicate the boundary of the palatal shelf (PS). Bar, 0.5 mm. (Y) Quantitative comparison of the size of the palatal shelves between control and *Dlx1/2*$^{-/-}$ mutant embryos at E11.5 and E13.5. *: $p<0.05$.

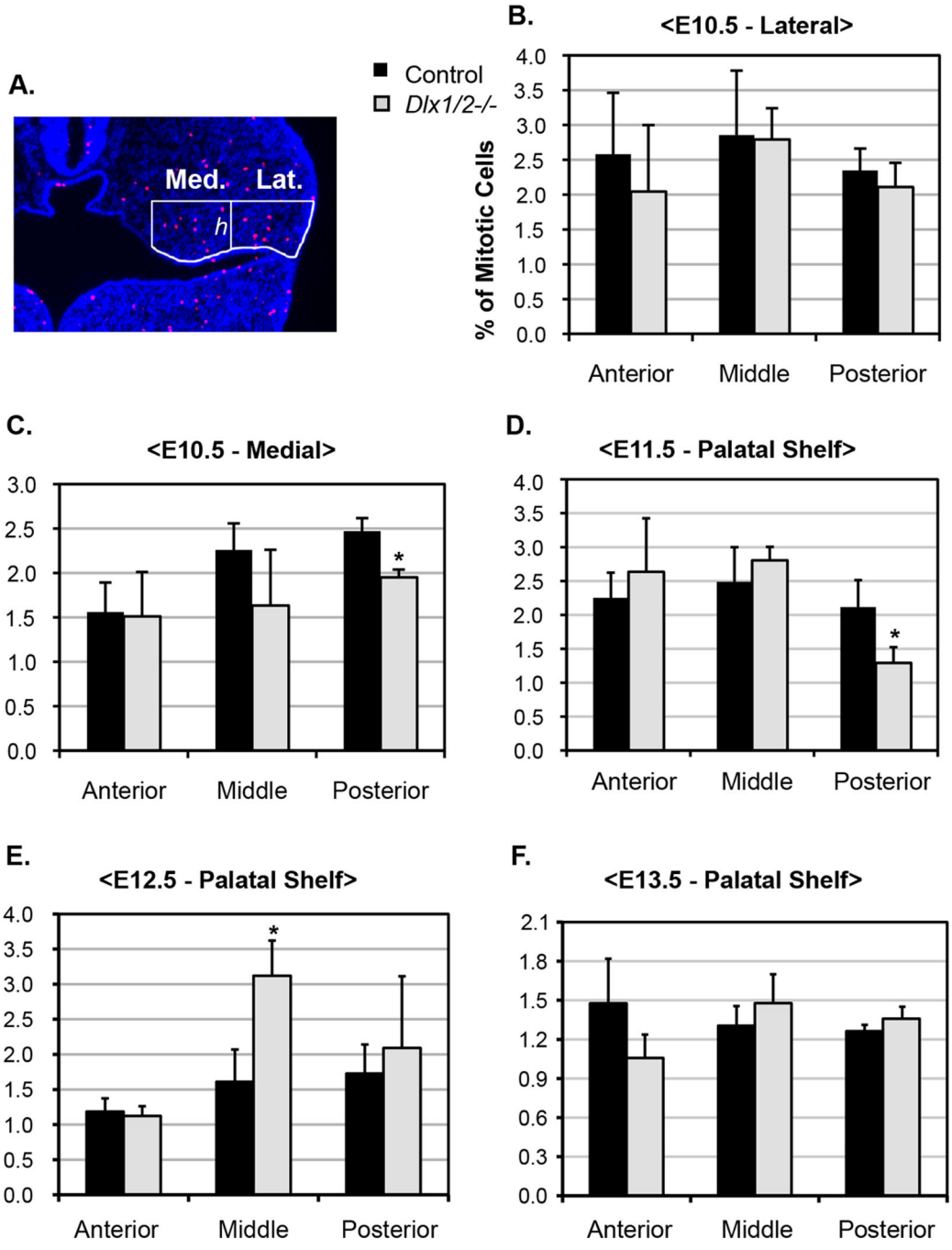

Figure 3. Cell proliferation analysis of the developing palate of *Dlx1/2*$^{-/-}$ mutants

(A) A representative image of E10.5 sections used for the quantitative analysis. A coronal section of the head at the posterior level was stained with anti-phosphohistone H3 antibody to detect mitotic cells (red) and with DAPI to detect all the nuclei (blue). The ventral domain of mxPA1 was divided into medial (med.) and lateral (lat.) halves as indicated, where *h* was kept constant for all the sections. (B–F) Quantitative comparison of the mitotic index between control and *Dlx1/2*$^{-/-}$ mutant embryos at E10.5–E13.5 as indicated. *: $p<0.05$.

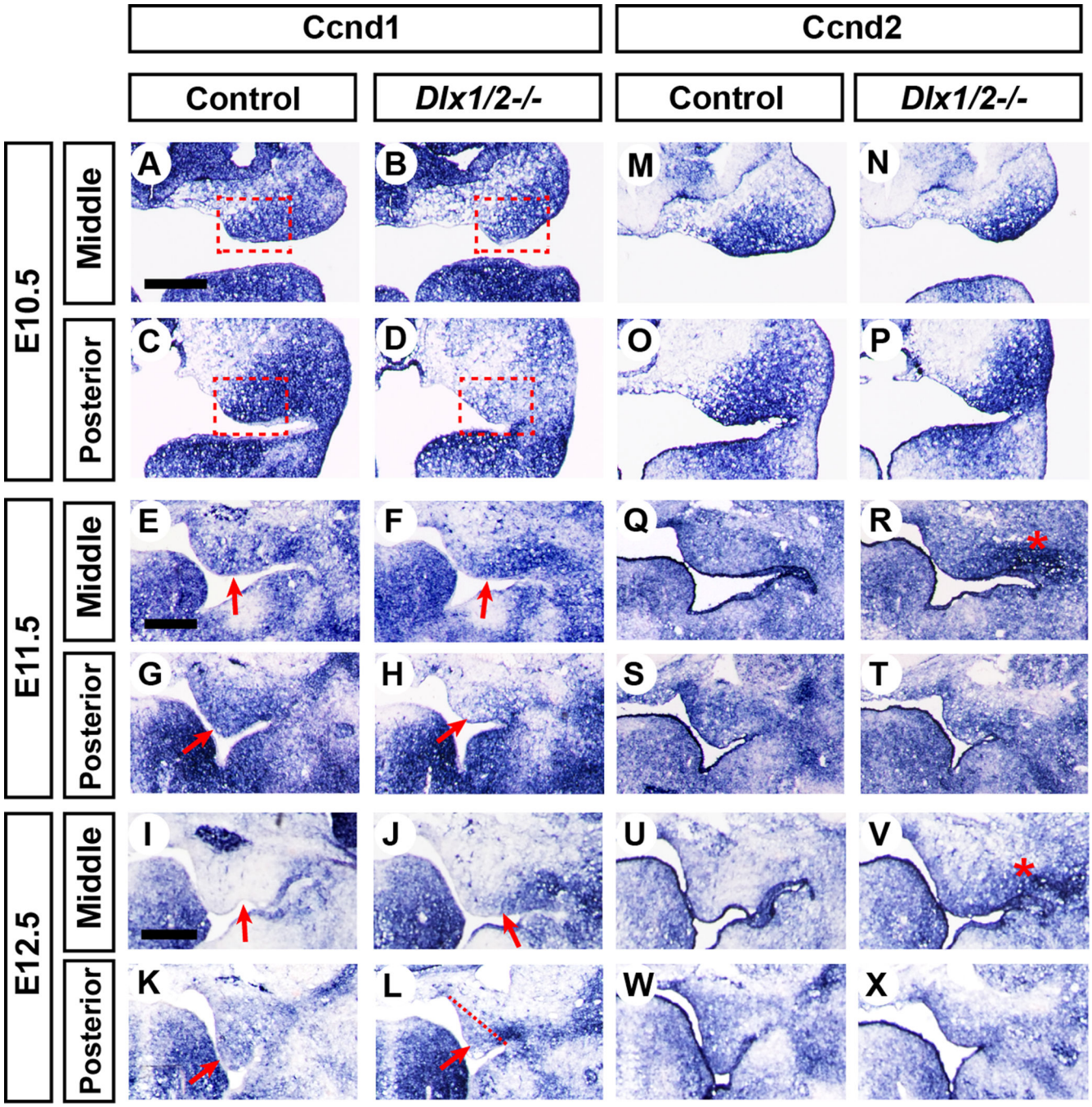

Figure 4. Expression of *Ccnd1* and *Ccnd2* during early palate development

Coronal sections of the orofacial region of control and *Dlx1/2*$^{-/-}$ mutant embryos processed by section in situ hybridization. The probes and the stages of the embryos are as indicated in the figure. The boxes in A–D indicate prospective palate domains within mxPA1. The arrows in E–L point to palatal shelves. The dotted line in L indicates the boundary of the palatal shelf. * in R and V indicates the site of ectopic cartilage development in the mutants. Bar, 0.25 mm.

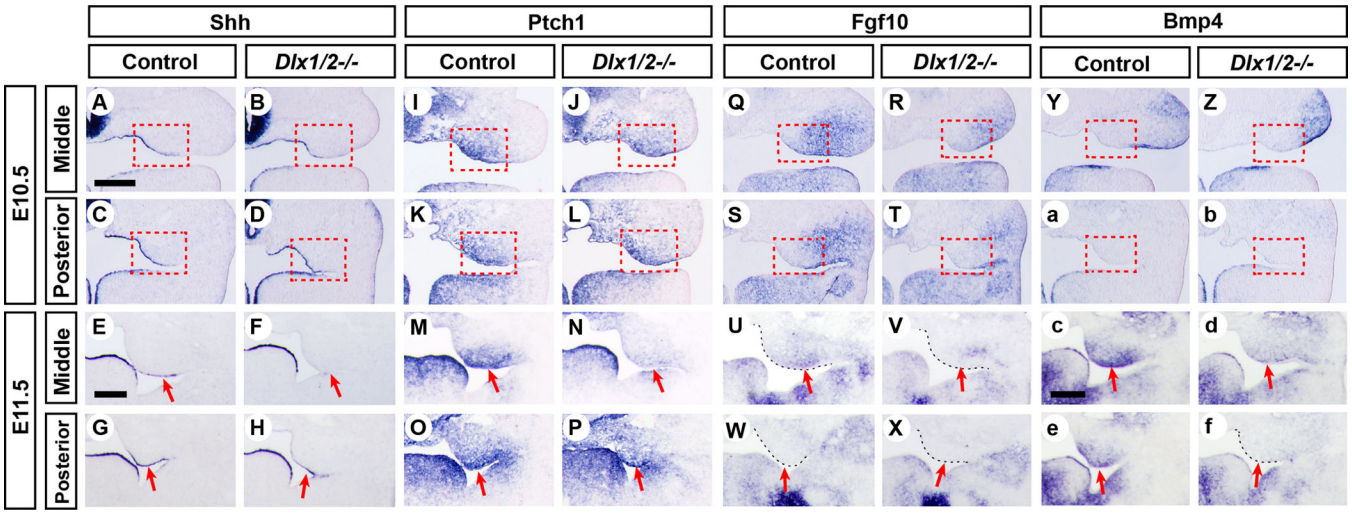

Figure 5. Expression of signaling molecules during early palate development

Coronal sections of the orofacial region of control and *Dlx1/2*$^{-/-}$ mutant embryos processed by section in situ hybridization. The probes and the stages of the embryos are as indicated. The boxes in A–D, I–L, Q–T, Y-b indicate prospective palate domains within mxPA1. The arrows in E–H, M–P, U–X, c–f point to palatal shelves. Bar, 0.25 mm.

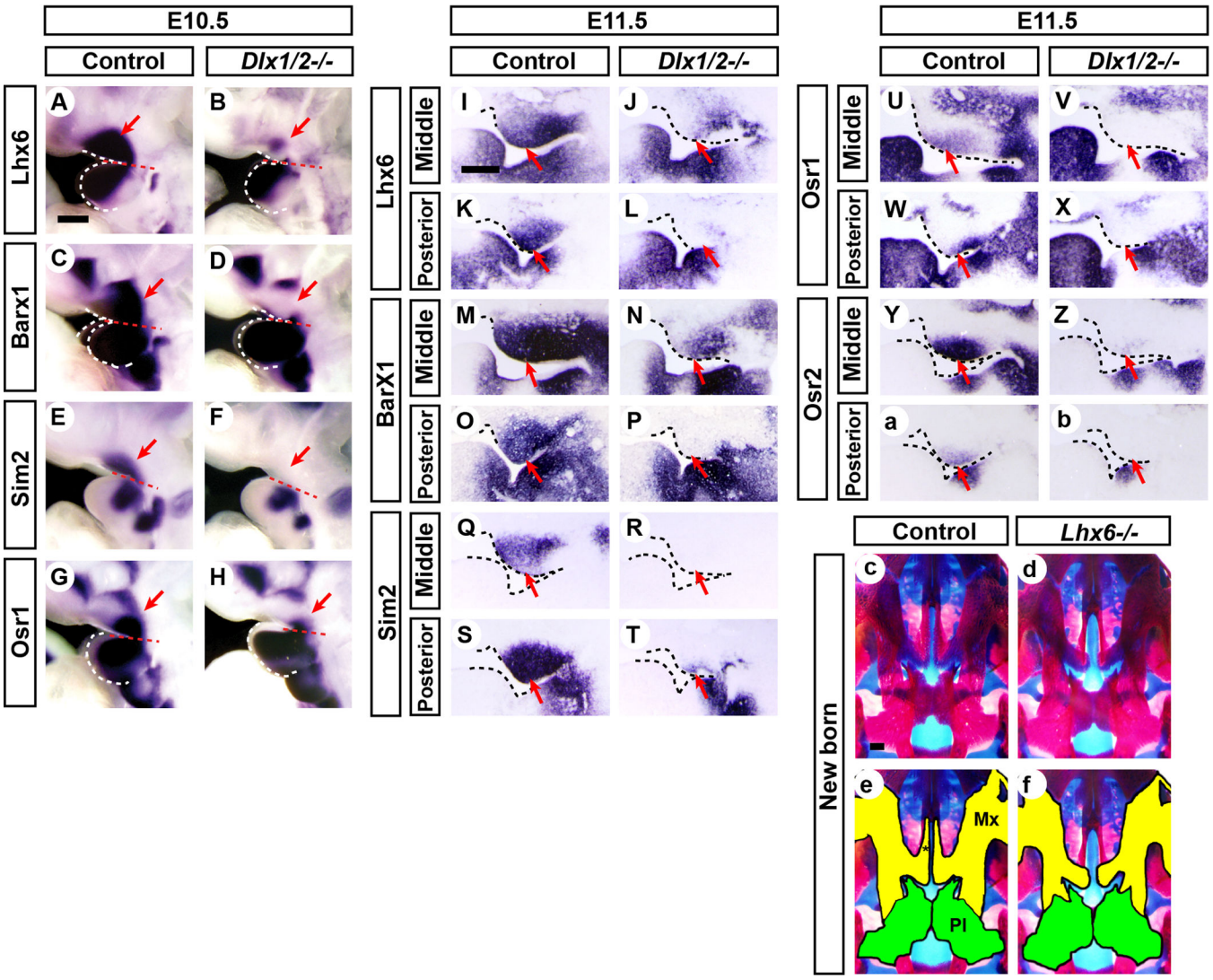

Figure 6. Abnormal expression of transcription factors in *Dlx1/2*$^{-/-}$ mutants and the palate defect of *Lhx6*$^{-/-}$ mutants

(A–H) Lateral views of the heads of E10.5 embryos processed by whole mount in situ hybridization. The probes and genotypes of the embryos are as indicated in the figure. The arrows point to mxPA1. (I-b) Coronal sections of the orofacial region of E11.5 embryos processed by section in situ hybridization. The probes and genotypes of the embryos are as indicated in the figure. The arrows point to the palatal shelves. (c,d) Skeleton preparations of new-born animals. The palatal views of the skull, after the lower jaw has been removed, are presented. (e,f) The same images as c,d, with yellow and green colors highlighting the two skeletal components of the hard palate, namely, the maxilla (Mx) and palatine (Pl). * in e indicates the palatal process of maxilla. Bar, 0.25 mm.

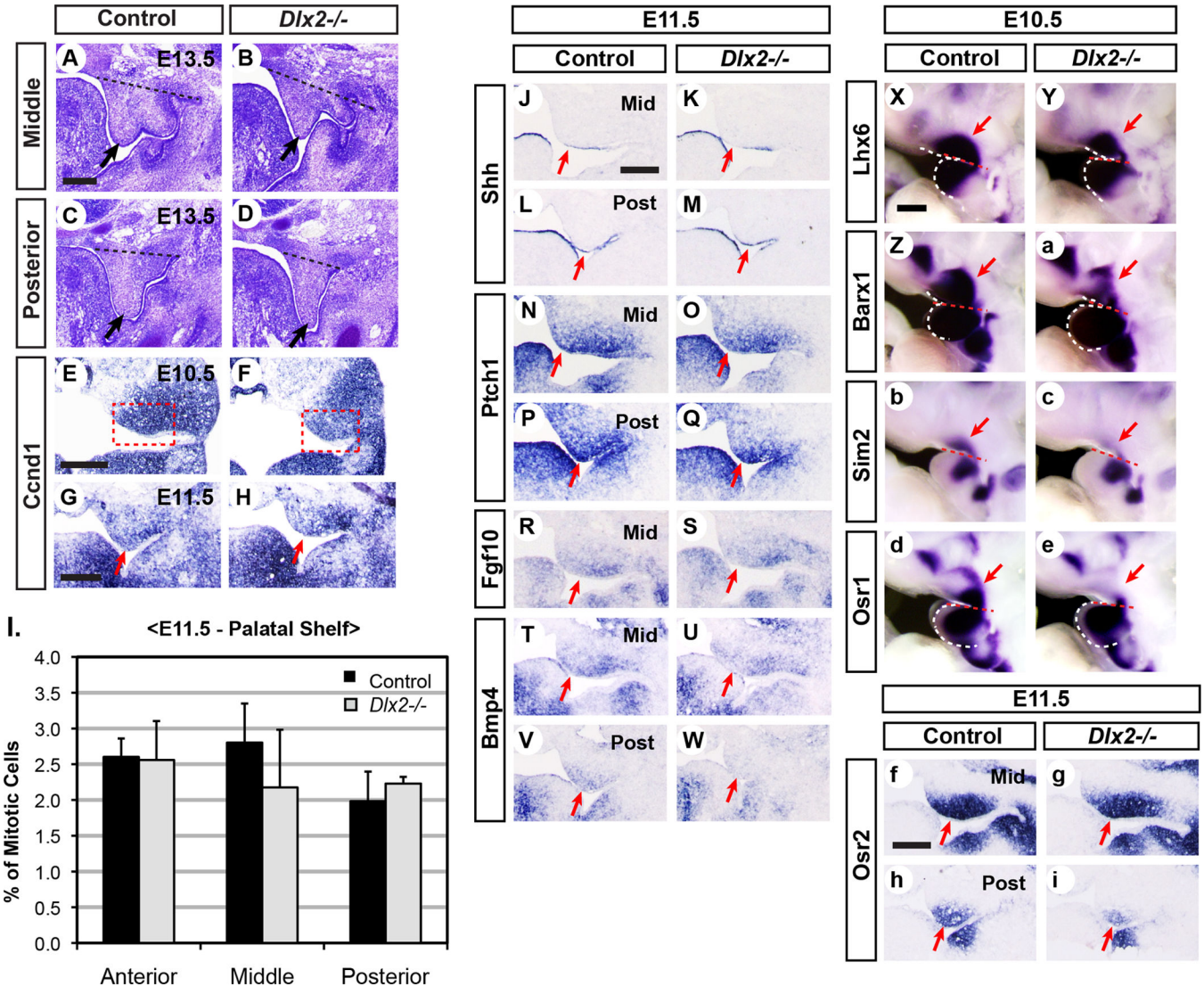

Figure 7. Analysis of *Dlx2*$^{-/-}$ mutant palate phenotype

(A–D) Coronal sections of the orofacial region of E13.5 control and *Dlx2*$^{-/-}$ mutant embryos stained with cresyl violet. The arrows point to the palatal shelves, and the dotted lines indicate the boundary of the palatal shelf. (E–H) Coronal sections of the (prospective) palate region of E10.5 (E,F) and E11.5 (G,H) control and *Dlx2*$^{-/-}$ mutant embryos processed with section in situ hybridization for *Ccnd1*. The sections are from the posterior level. The boxes in E,F indicate prospective palate region, and arrows in G,H point to the palatal shelves. (I) Quantitative comparison of the mitotic index between control and *Dlx2*$^{-/-}$ mutants at E11.5. (J–W, f–i) Coronal sections of the orofacial region of E11.5 embryos processed with section in situ hybridization. The probes and genotypes of the embryos are as indicated in the figure. Arrows point to palatal shelves. Mid, middle level; Post, posterior level. (X-e) Lateral views of the heads of E10.5 embryos processed by whole mount in situ hybridization. The probes and genotypes of the embryos are as indicated in the figure. The arrows point to mxPA1. Bar, 0.25 mm.

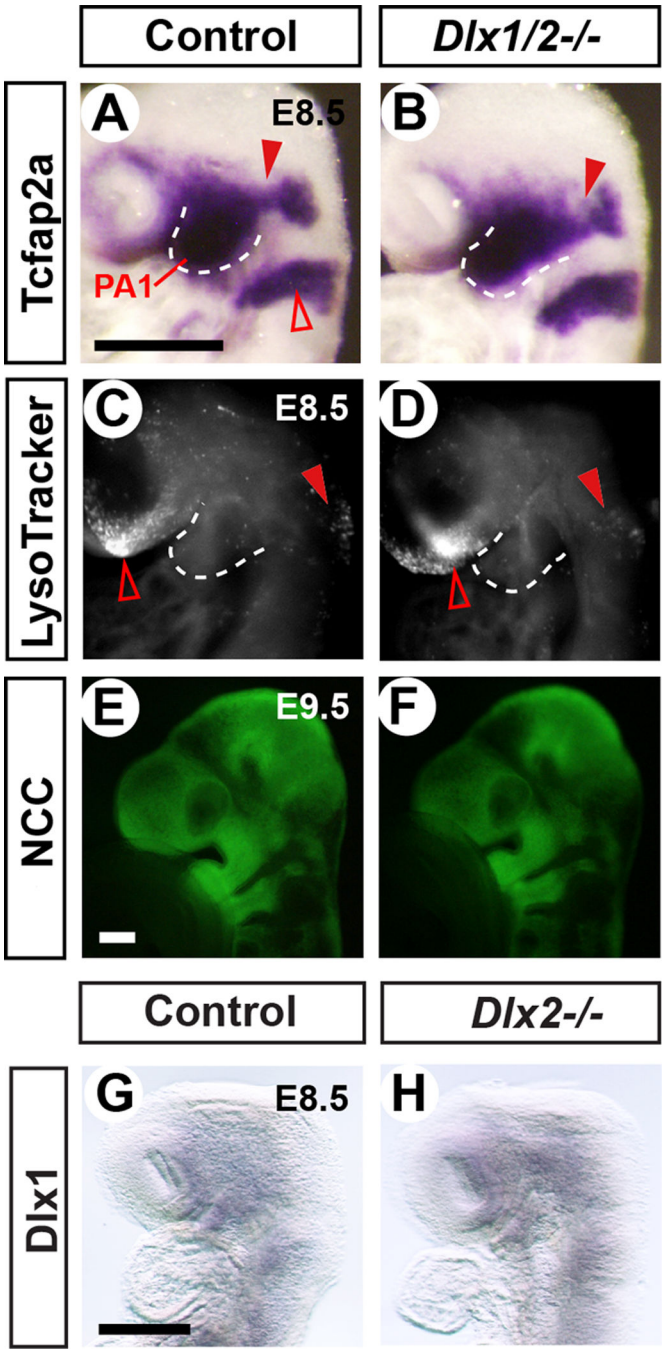

Figure 8. Migration of the cranial neural crest cells (CNCCs) into PA1 appears unaffected in *Dlx1/2*$^{-/-}$ mutants, and there is no compensatory up-regulation of *Dlx1* in migrating CNCCs of *Dlx2*$^{-/-}$ embryos

(A,B) E8.5 (12 somite stage) embryos were processed by whole mount in situ hybridization. Arrowheads point to the stream of CNCCs migrating toward PA1. The open arrowhead in A points to CNCCs that will contribute to PA2. (C,D) E8.5 (12 somite stage) embryos were stained with LysoTracker to detect cell death. No significant cell death was observed in CNCCs in and around PA1, in either control or *Dlx1/2*$^{-/-}$ embryos. Arrowheads indicate death in CNCCs from rhombomere 3, which occurs during normal development. Open

arrowheads point to cell death in the anterior neural ridge. (E,F) E9.5 (25 somite stage) embryos showing the distribution of CNCCs (green) via Wnt1-Cre reporter system. The exact genotypes of the embryos are *Wnt1-Cre;Dlx1/2*$^{+/-}$*;R26R*$^{EYFP/+}$ (E) and *Wnt1-Cre;Dlx1/2*$^{-/-}$*;R26R*$^{EYFP/+}$ (F). (G,H) Lateral views of the heads of E8.5 (12 somite stage) embryos processed by whole-mount in situ hybridization. *Dlx1* is not expressed at this stage in either control or *Dlx2*$^{-/-}$ embryos.